Molecular Pharmacology Fast Forward. Published on February 18, 2005 as doi:10.1124/mol.104.007435
This article has not been copyedited and formatted. The final version may differ from this version.

Title page

Developmental regulation of β-carboline-induced inhibition of glycine-evoked responses depends on glycine receptor β subunit expression[£]

Jean-Marie MANGIN[*], Laurent NGUYEN[*], Catherine GOUGNARD, Grégory HANS, Bernard ROGISTER, Shibeshih BELACHEW, Gustave MOONEN, Pascal LEGENDRE[*] and Jean-Michel RIGO[*]

Center for Cellular and Molecular Neuroscience, University of Liège, 17 place Delcour, B-4020 Liège, Belgium

Molecular Pharmacology Fast Forward. Published on February 18, 2005 as DOI: 10.1124/mol.104.007435
This article has not been copyedited and formatted. The final version may differ from this version.

Running title page

Running title

β-carboline inhibition of the glycine receptor

Corresponding author

Jean-Michel RIGO, Department of Physiology, Transnationale Universiteit Limburg / Limburgs Universitair Centrum, Biomedisch Onderzoekinstituut, B-3590 Diepenbeek, Belgium, telephone: +32 11 26 85 36, fax: +32 4 375 82 55, e-mail: jeanmichel.rigo@luc.ac.be

Numbers

Text pages: 44

Tables: 1

Figures: 8

References: 52

Words in abstract: 254

Words in introduction: 643

Words in discussion: 1154

Nonstandard abbreviations

βCCB: n-butyl-β-carboline-3-carboxylate; ANOVA-1: one-way analysis of variance; ANOVA-2: two-ways analysis of variance; CHO cells: Chinese hamster ovarian cells; DIV: days *in vitro*; DMCM: methyl-6,7-dimethoxy-4-ethyl-β-carboline-3-carboxylate; FG7142: n-methyl-β-carboline-3-carboxamide; $GABA_AR$: type A γ-aminobutyric acid receptor; GlyR: glycine receptor

Molecular Pharmacology Fast Forward. Published on February 18, 2005 as DOI: 10.1124/mol.104.007435
This article has not been copyedited and formatted. The final version may differ from this version.

Abstract

In this work, we show that β-carbolines, which are known negative allosteric modulators of $GABA_A$ receptors, inhibit glycine-induced currents of embryonic mouse spinal cord and hippocampal neurons. In both cell types, β-carboline-induced inhibition of glycine receptor (GlyR)-mediated responses decreases with time in culture. Single-channel recordings show that the major conductance levels of GlyR unitary currents shifts from high levels (≥ 50 pS) in 2-3 DIV neurons to low levels (< 50 pS) in 11-14 DIV neurons, assessing the replacement of functional homomeric GlyR by heteromeric GlyR. In cultured spinal cord neurons, the disappearance of β-carboline inhibition of glycine responses and high conductance levels is almost complete in mature neurons whereas a weaker decrease in β-carboline-evoked glycine response inhibition and high conductance level proportion is observed in hippocampal neurons. To confirm the hypothesis that the decreased sensitivity of GlyR to β-carbolines depends on β subunit expression, CHO cells were permanently transfected either with GlyR α2 subunit alone or in combination with GlyR β subunit. Single channel recordings revealed that the major conductance levels shifted from high levels (≥ 50 pS) in GlyR-α2-transfected cells to low levels (< 50 pS) in GlyR-α2+β-containing cells. Consistently, both picrotoxin- and β-carboline-induced inhibition of glycine-gated currents were significantly decreased in GlyR-α2+β-transfected cells compared to GlyR-α2-containing cells. In summary, we demonstrate that the incorporation of β subunits in GlyRs confers resistance not only to picrotoxin- but also to β-carboline-induced inhibition. Furthermore, we also provide evidence that hippocampal neurons undergo *in vitro* a partial maturation process of their GlyR-mediated responses.

Molecular Pharmacology Fast Forward. Published on February 18, 2005 as DOI: 10.1124/mol.104.007435
This article has not been copyedited and formatted. The final version may differ from this version.

Introduction

In the mammalian central nervous system (CNS), fast inhibitory neurotransmission is mediated by two major classes of ligand-gated channels, namely type A γ-aminobutyric acid receptors ($GABA_ARs$) and strychnine-sensitive glycine receptors (GlyRs) (Moss and Smart, 2001). While GABAergic neurotransmission has a widespread distribution throughout the brain, glycinergic transmission is mainly restricted to the spinal cord and to the brainstem where it controls motor rhythm generation underlying the locomotor behavior and also coordinates spinal reflexes (Legendre, 2001). GlyRs are however also present in various upper brain regions (Malosio *et al.*, 1991), including the cerebellum (Virginio and Cherubini, 1997), the cortex (Flint *et al.*, 1998), the striatum (Sergeeva and Haas, 2001), the amygdala (McCool and Farroni, 2001), the hippocampus (Mori *et al.*, 2002;Chattipakorn and McMahon, 2003;Thio *et al.*, 2003), the ventral tegmental area (Ye, 2000) or the substantia nigra (Mangin *et al.*, 2002). In some of those regions, GlyRs do not seem to participate in fast transmission, but rather in tonic modulation of excitability (Chattipakorn and McMahon, 2003;Mori *et al.*, 2002).

GlyRs share with the other members of the nicotinic super-family of ligand-gated channels a pentameric structure (Ortells and Lunt, 1995). Four α subunits (α1-α4) have been so far characterized for the GlyR (Legendre, 2001). They are able to form functional homomeric channels both *in vivo* (Singer and Berger, 2000;Thio *et al.*, 2003) and in expression systems (Beato *et al.*, 2004;Mangin *et al.*, 2003). They moreover carry all the binding sites for GlyR agonists (Legendre, 2001). Conversely, only one β subunit is known which has no binding sites for GlyR ligands, but rather bind the intracellular anchoring protein gephyrin (Schrader *et al.*, 2004). In the adult brainstem and spinal cord, it is now widely accepted that GlyRs mainly consist of α1β heteromers with 3 α1 subunits and 2 β (Singer and Berger, 2000). As for the vast

Molecular Pharmacology Fast Forward. Published on February 18, 2005 as DOI: 10.1124/mol.104.007435
This article has not been copyedited and formatted. The final version may differ from this version.

majority of ligand-gated channels, a developmental regulation of GlyR subunit expression is known to occur and is associated with changes in the functional properties of the so-formed receptor. In that respect, in the spinal cord and in the brainstem, embryonic GlyRs are mainly α2 homomers that are transiently replaced by α2β heteromers around birth ('juvenile' stage) before to switch to the adult form, namely α1β heteromers (Singer and Berger, 2000;Tapia and Aguayo, 1998;Withers and St John, 1997).

Compared to $GABA_A$Rs, fewer modulators of the GlyRs have been characterized (Laube *et al.*, 2002). Among the main antagonists, strychnine is a pro-convulsive alkaloid specific for all GlyR variants and picrotoxin, which is a channel blocker of $GABA_A$Rs, is a competitive allosteric antagonist with a higher efficacy at GlyR homomers than at heteromers (Lynch *et al.*, 1995). Other documented modulators at the GlyR include physiological agents (zinc (Suwa *et al.*, 2001) and protons (Chen *et al.*, 2004)) and various pharmacological drugs which often also interact with other channels, *e.g.* anesthetics, alcohols, steroids, dihydropyridines or tropeins (Laube *et al.*, 2002).

In a previous study (Rigo *et al.*, 2002), it has been mentioned that glycine-induced responses mediated by GlyRs could be reversibly antagonized by β-carbolines in cultured mouse spinal cord neurons 2-4 days after plating. β-carbolines are better known as negative allosteric modulators of the benzodiazepine site of $GABA_A$Rs (Teuber *et al.*, 1999). Since GlyR inhibition by β-carbolines was described in very 'immature' neurons, this suggested that β-carbolines could preferentially act on α homomers, the immature form of the receptor.

The goal of our study is to determine if β-carboline-evoked inhibition of GlyR depends on the expression of GlyR β subunit. By means of electrophysiological, pharmacological and molecular biology techniques, we demonstrate that β-carbolines are antagonists at α homomers, but not at αβ heteromeric GlyRs. We also show that cultured hippocampal neurons also undergo,

as cultured spinal cord neurons, an *in vitro* maturation characterized by an increased expression of functional heteromeric GlyRs.

Part of this work had been previously published in abstract form (Rigo *et al.*, 1998).

Molecular Pharmacology Fast Forward. Published on February 18, 2005 as DOI: 10.1124/mol.104.007435
This article has not been copyedited and formatted. The final version may differ from this version.

Materials and methods

The experiments have been carried out in accordance with the Declaration of Helsinki and conform to the European Community guiding principles in the care and use of animals (86/609/CEE, CE off J n°L358, 18 December 1986), the French decree n°97/748 of October 19, 1987 (*J. Off. République Française*, 20 October 1987, pp. 12245-12248) and the recommendation of CNRS and University Paris VI.

Neuronal cell cultures

Spinal cord neurons and hippocampal neurons were obtained, respectively, from 13-day-old and 16-day-old mouse embryos using methods fully described previously (Withers and St John, 1997;Leprince *et al.*, 1989). Briefly, spinal cords or hippocampi were carefully dissected and freed of meninges. They were then cut into small fragments which were incubated in trypsin (0.25%) and deoxyribonuclease (0.1%) in Ca^{2+}-Mg^{2+} free salt solution for 25 min at 37°C. This was followed by a wash with their culture medium which consisted of Dulbecco's modified minimum essential medium (Invitrogen, Gent, Belgium) supplemented with glucose (6 g/l, final concentration), 5% (V/V) foetal calf serum (Invitrogen), 10% (V/V) horse serum (Invitrogen) and the N1 supplement (insulin 5 μg/ml; transferrin 5 μg/ml; progesterone 20 nM; putrescine 100 μM, selenium 30 nM). Dissociation was obtained by up and down aspirations through the large tip of a 5 ml plastic pipette put on the bottom of a conical glass tube. The resulting cell suspension was filtered through a 40 μm nylon sieve. Fifty microliters of the cell suspension was seeded on polyornithine (0.1 mg/ml in distilled water) coated glass coverslips (10 mm diameter) in the centre of 35 mm plastic Petri dishes (NUNC, Roskilde, Denmark) at a concentration of 1.25×10^6 cells per ml. The medium was renewed once weekly and cells were used for electrophysiological

Molecular Pharmacology Fast Forward. Published on February 18, 2005 as DOI: 10.1124/mol.104.007435
This article has not been copyedited and formatted. The final version may differ from this version.

recordings after 2-17 days-*in-vitro* (DIV). In the results, different culture time periods are differentiated: 'young' or 'immature' neurons correspond to neurons cultivated for less than 4 DIV, *i.e.* for 2 to 3 DIV, which are noted '< 4 DIV' in the figures and 'old' or 'mature' neurons correspond to neurons cultured for more than 7 DIV, *i.e.* for 8 to 15 DIV in the case of spinal cord neurons and for 10 to 17 DIV in the case of hippocampal neurons, which are noted '> 7 DIV' in the figures.

CHO cells cultures

Chinese Hamster Ovarian cell (CHO-K1, ATCC n° CCL61) were cultured in 6-well plates in minimum essential medium (Invitrogen) supplemented with 10% (V/V) fetal calf serum (Invitrogen). CHO were sub-cultured two times per week. For electrophysiological recordings, cells were seeded onto glass coverslips coated with poly-ornithine (0.1 mg/ml).

RT-PCR and quantitative RT-PCR

Total RNAs from adult mouse brains and from cultured neurons and transfected CHO cells were extracted and purified using a mini RNeasy kit (Qiagen, Westburg, The Netherlands). As determined by 260/280 OD readings, 1 µg of total RNA was reverse-transcribed using primers with oligodT and 200 U of reverse transcriptase (Superscript II, Invitrogen). A 2 µl aliquot of the resulting cDNA reaction, used as template, was added to a 50 µl PCR reaction mixture containing: 0.5 µM of both forward and reverse primers synthesized by Eurogentec (Seraing, Belgium) (see **table 1**), 0.2 mM of each dNTP, 1.5 mM of $MgCl_2$ and 5 U of Taq polymerase (Promega, The Netherlands). Moreover, 5% of DMSO was added to the reaction in the PCR mixture containing the β primers. The PCR program was achieved in a PTC 200 instrument (MJ Research, Waltham, MA, UA). After a 3 min denaturation step at 94°C,

Molecular Pharmacology Fast Forward. Published on February 18, 2005 as DOI: 10.1124/mol.104.007435
This article has not been copyedited and formatted. The final version may differ from this version.

amplifications were carried out for 33 cycles (94°C for 30 s, 60°C for 15 s and 72°C for 30 s), followed by a final extension at 72°C for 9 min. Please note that we used 55°C for the annealing of α1 primers. In the case of α3, after a 2 min denaturation step at 94°C, we performed 34 cycles (94°C for 48 s, 58°C for 60 s and 72°C for 90s) and a final extension step at 72°C for 5 min. The amplification program for β was an initial denaturation step at 95°C for 2 min then 2 cycles (94°C for 45 s, 50°C for 30s and 72°C for 30 s) followed by two identical cycles except that the annealing temperature was 52°C, then followed by two other identical cycles with an annealing temperature of 54°C and then 21 cycles where annealing temperature was 56°C. The β PCR was finished by a final extension step at 72°C for 5 min. Ten microliters of the PCR reaction were analysed in a 2% agarose gel in tris-acetic acid-EDTA (TAE) buffer. Quantitative PCR was carried out using standard protocols with Quantitec SYBR Green PCR Kit (Qiagen). The PCR mix contained SYBR Greeen Mix, 0.5 µM primers (**table 1**), 1 ng DNA template and nuclease-free water to reach a final volume of 25 µl. Quantitative PCRs were performed on RotorGene RG-3000 (Corbett Research, Westburg, The Netherlands) and analyzed with the Rotorgene Software (Corbett Research). The percentage of β subunit gene expression by cultured spinal cord neurons was normalized in function of actin gene expression and was compared to the gene expression in 15 DIV spinal cord neurons that was considered as 100 %.

<< Table 1 should be placed here >>

GlyR α2 and β subunit cloning and transfection

1 µg of total RNAs extracted from spinal neurons in culture were reversely transcribed in a 20 µl reaction volume using Superscript (Invitrogen) and oligodT as primers. Two microliters of the obtained cDNA was used as template in a PCR reaction containing 2,5 U of High Fidelity enzyme blend (Roche, Brussels, Belgium), 1.5 mM of $MgCl_2$, the forward primer

Molecular Pharmacology Fast Forward. Published on February 18, 2005 as DOI: 10.1124/mol.104.007435
This article has not been copyedited and formatted. The final version may differ from this version.

(ATCACGGAAACAGGAATGAAC) and the reverse primer (CATCTATTTCTTGTGGACATC) for the α2A splice variant of the GlyR α2 subunit (acces # X61159). The PCR reaction was performed in a MJ-Research PTC-200 thermal cycler (after a 2 minutes denaturation initial step, 10 cycles at 94°C for15 sec, at 50°C for 30 sec and at 72°C for 2 minutes were followed by 20 cycles at 94°C for15 sec, at 60°C for 30 sec and at 72°C for 2 minutes with 5 additional seconds per cycle and a final extension step at 72°C for 2 minutes). PCR product was purified on agarose gel and cloned in a pCRII-TOPO vector (InVitrogen). The sequence was checked and the GlyR α2 subunit was then subcloned in pTRACER-CMV vector (InVitrogen) in BstXI sites. The various constructs and their orientation were checked by sequencing. The constructs were transfected into CHO cells using the DAC30 lipofection reagent (Eurogentec, Liège, Belgium) selected with Zeocin 500 µg/ml 48 hours later (Invitrogen). Selected recombinant CHO cells were then cloned by dilution and several clones were tested for their expression of functional GlyRs by RT-PCR, immunocytochemistry and electrophysiology. The clone that was selected for its higher expression level of GlyR α2 subunits is hereafter denoted GlyR-α2. The GlyR β subunit was also cloned by RT-PCR from cultured spinal neuron RNA using primer with an ApaI site underlined (Forward: AACGGGCCCGTTTTCAAGATGAAGTTTTCGTTG and reverse: TTCGGGCCCTAAATATATAGACC). The resulting PCR product was purified on agarose gel and cloned in a pCRII-TOPO vector (InVitrogen). The GlyR β subunit was then subcloned in pCDNA3-Myc-His vector in ApaI sites. The various constructs and their orientation were checked by sequencing. The constructs were transfected into CHO-GlyR-α2 cells using the DAC30 lipofection reagent (Eurogentec, Liège, Belgium) and selected with G418 at 500µg/ml 48 hours later (Invitrogen). Selected recombinant CHO-GlyR-α2+β cells were tested as described above. The selected clone used in this study is hereafter denoted GlyR-α2+β.

Molecular Pharmacology Fast Forward. Published on February 18, 2005 as DOI: 10.1124/mol.104.007435
This article has not been copyedited and formatted. The final version may differ from this version.

Immunocytochemistry

CHO cells were fixed with 4% (V/V) paraformaldehyde in PBS for 10 minutes at room temperature. Cells were then permeabilized in PBS+0.3% Triton for 10 min and non-specific binding was subsequently blocked by a 30 minutes treatment in a PBS solution containing 0.25% gelatin (PBSg). To reveal the GlyR mAb4a epitope, cells were then immersed in methanol for 10 min at –20°C. Cells were incubated overnight at 4°C with mouse anti-GlyR α subunit mAb4a (staining an epitope common to all GlyR α subunits; Alexis Biochemicals, Lausen, Switzerland) at 1:100 in PBSg . Cells were then incubated during 2 hours at room temperature in a rhodamine-conjugated anti-mouse immunoglobulin (Jackson Immunoresearch Laboratories, West Grove, USA) diluted at 1:500 in PBSg. Three rinses in PBS were performed between all different steps. Preparations were mounted in Vectashield (Vector Laboratories, CA, USA). In the control experiments, where primary antibodies were omitted, no detectable immunofluorescence was observed. Images were acquired using a laser scanning confocal microscope (MRC1024, BioRad, Hertfordshire, UK).

Electrophysiology

Whole-cell recordings and drugs

Coverslips containing cultured neurons or transfected CHO cells were transferred to the stage of a Zeiss interferential contrast microscope. They were maintained at room temperature (20-25°C) in a recording chamber which was continuously perfused with a physiological saline solution containing (in mM): NaCl, 116; D-glucose, 11.1; KCl, 5.4; $CaCl_2.2H_2O$, 1.8; $MgCl_2.6H_2O$, 2.0; HEPES, 10.0; pH 7.2. Glycine was purchased from UCB (Brussels; Belgium).

Molecular Pharmacology Fast Forward. Published on February 18, 2005 as DOI: 10.1124/mol.104.007435
This article has not been copyedited and formatted. The final version may differ from this version.

GABA, strychnine, picrotoxin, bicuculline methiodide, SR-95531 (gabazine), Ro 15-1788 (flumazenil), methyl-6,7-dimethoxy-4-ethyl-β-carboline-3-carboxylate (DMCM), n-butyl-β-carboline-3-carboxylate (βCCB) and n-methyl-β-carboline-3-carboxamide (FG 7142) were purchased from Sigma (USA). Stock solutions were prepared at 500 times their final concentration in tridistilled water (GABA, glycine, strychnine and gabazine) or in DMSO (picrotoxin, flumazenil, DMCM, βCCB and FG 7142). In the latter case, 0.2% DMSO were also included in other conditions, but did not significantly influence glycine-gated currents (data not shown). All the drugs were applied by means of a local microperfusion system (SPS-8, List Medical). Borosilicate patch-clamp recording electrodes (5-10 MΩ) were made using a Flaming-Brown microelectrode puller (P97, Sutter Instrument Co). Micropipettes were filled with an intracellular-like solution containing (in mM): KCl, 130.0; $CaCl_2.2H_2O$, 1.0; D-glucose, 11.1; EGTA, 10.0; Na_2-ATP, 2.5; Mg-ATP, 2.5; HEPES, 10.0, pH 7.4. Standard whole-cell recordings were performed with a Bio-Logic RK400 patch-clamp. Series resistances (10-20 Ω) were electronically compensated (80 to 85%) and current traces were filtered at 3 kHz, acquired and digitized at 0.5 kHz, and stored on a personal computer system. Control of drug application and data acquisition were achieved using an ITC-16 acquisition board (Instrutech Corporation) and the TIDA for Windows software (HEKA Elektronik Lombrecht/Pfolz, Germany).

Outside-out recordings

Standard outside-out recordings were achieved under direct visualization (Nikon Optiphot microscope). Cells were continuously perfused at room temperature (20°C) with bathing solution (2 ml/min) containing (in mM): NaCl, 145.0; KCl, 1.5; $CaCl_2$, 2.0; $MgCl_2$, 1.0; HEPES, 10.0; Glucose 15.0 (pH 7.3, osmolarity 330 mOsm). Patch-clamp electrodes were pulled from thick-wall borosilicate glass (5-10 MΩ). They were fire-polished and filled with (in mM): CsCl, 135;

Molecular Pharmacology Fast Forward. Published on February 18, 2005 as DOI: 10.1124/mol.104.007435
This article has not been copyedited and formatted. The final version may differ from this version.

MgCl2, 2; Na3ATP, 4; EGTA, 10; HEPES, 10 (pH 7.2, osmolarity 290 mOsm). Currents were recorded using an Axopatch 1D amplifier (Axon instruments, Foster City, USA) filtered at 10 KHz, and stored using a digital recorder (DAT DTR 1201, Sony, Tokyo, Japan). During recordings, values of seal resistance ranged from 2 to 20 GΩ and patches were recorded during 15-30 min after excision. Control and drug solutions were gravity-fed into two channels of a thin-wall glass theta tube (2 mm outer diameter; Hilgenberg) pulled and broken at a tip diameter of 200 µm. The drug application was performed by manually translating the patch pipette in front of the drug-containing channel.

Data analysis

Except when stated otherwise, the results are expressed as mean and standard error of the mean (SEM). For whole-cell recordings, "n" represented the number of recorded cells. Peak currents in the different experimental conditions were measured and subsequently normalized to the preceding and the following responses (100 %) in control conditions. Agonist concentration-response profiles were fitted to the following equation: $I/I_{max} = 1/(1+(EC_{50}/[agonist])n_h)$, where I and I_{max} respectively represent the agonist-induced current at a given concentration and the maximum current induced by a saturating concentration of the agonist. EC_{50} is the half-maximal effective agonist concentration and n_h is the Hill slope. Modulator concentration-response curves were fitted by a similar procedure and yielded IC_{50} values being half-maximal inhibitory drug concentrations.

For all experiments, a statistical analysis was performed using either unpaired two-tailed Student's *t*-test between control and experimental conditions or one-way analysis of variance (ANOVA-1) followed by a Dunnett's multiple comparison post-tests when significance was reached or two-ways analysis of variance (ANOVA-2) between concentration-response curves

Molecular Pharmacology Fast Forward. Published on February 18, 2005 as DOI: 10.1124/mol.104.007435
This article has not been copyedited and formatted. The final version may differ from this version.

(GraphPad Prism software, version 4.00, San Diego, CA). The level of significance was expressed as follows: * $P < 0.05$, ** $P < 0.01$, and *** $P < 0.001$.

For outside-out recordings, the analysis of the evoked single-channel openings was performed by selecting patches with a low frequency of openings to avoid overlapping events. Single-channel current levels were determined using point-per-point amplitude histograms obtained from recording epochs of 25-50 seconds. Amplitude histograms were fitted with a sum of Gaussian functions, using the least square method (Simplex algorithm). The optimal number of Gaussian functions was determined by comparing the sum of squared errors (SSE) of the different multi-Gaussian fits. The different conductance levels were defined from the mean current amplitude of each Gaussian function and the theoretical E_{Cl} (-2 mV). The relative proportion of time spent in each level was given by the relative area of each Gaussian function. Open times were analyzed manually using Axograph 4.6 software (Axon Instruments, USA).

Molecular Pharmacology Fast Forward. Published on February 18, 2005 as DOI: 10.1124/mol.104.007435
This article has not been copyedited and formatted. The final version may differ from this version.

Results

β-carbolines dose-dependently inhibit glycine-gated currents in *in vitro* cultured spinal cord neurons

In the whole-cell configuration of the patch-clamp technique and in voltage-clamp mode at a holding potential of -70 mV, we recorded in 2-3 DIV cultured spinal cord neurons inward currents elicited by bath application (10 s) of GABA and of glycine (**figures 1A** and **1B**). These inward currents reversed around 0 mV (data not shown), consistent with them being carried mainly by Cl^- ions, the calculated Nernst equilibrium potential of chloride being 0.6 mV. GABA currents were blocked in the presence of either bicuculline methiodide, gabazine or picrotoxin, and glycine responses were inhibited by strychnine (data not shown), indicating the activation of ionotropic $GABA_A$ and glycine receptors, respectively. Throughout this paper, glycine currents were recorded in the presence of 10 µM bicuculline methiodide and GABA responses in the presence of 1 µM strychnine to avoid cross activation.

<< Figure 1 should be placed here >>

As shown in **figures 1B** and **1C**, and as already partially reported (Rigo *et al.*, 2002), β-carbolines (n-butyl-β-carboline-3-carboxylate, βCCB; methyl-6,7-dimethoxy-4-ethyl-β-carboline-3-carboxylate, DMCM; n-methyl-β-carboline-3-carboxamide, FG7142) dose-dependently and reversibly inhibited the current gated by 100 µM glycine, a concentration close to its EC_{50} on these neurons (77.7 ± 13.6 µM, n = 8). The level of inhibition by 100 µM βCCB of glycine-induced currents (40.9 ± 5.8 % of control, n = 11) was in the same order as for GABA-gated responses (38.9 ± 4.8 % of control, n = 5; P = 0.8, unpaired t-test), its classical target (**figures 1A** and **1B**). The plots of the relative current amplitudes as a function of β-carboline

Molecular Pharmacology Fast Forward. Published on February 18, 2005 as DOI: 10.1124/mol.104.007435
This article has not been copyedited and formatted. The final version may differ from this version.

concentrations were best fitted by Hill equations yielding half-maximal inhibitory concentrations (IC_{50}) for βCCB of 11.5 ± 2.8 µM (n = 3-15), for DMCM of 15.8 ± 2.8 µM (n = 3-26) and for FG7142 of 46.2 ± 24.2 µM (n = 4-8). Since these concentration-response curves did not statistically differ (P = 0.09, ANOVA-2), βCCB was preferentially used to allow inter-model comparisons and, hence, illustrated in subsequent figures.

In vitro maturation-dependent expression of GlyR β subunit confers spinal cord neurons resistance to β-carboline-induced inhibition of glycine-gated currents

It is well known that a developmental switch in GlyR subunits does occur during spinal cord development both *in vivo* (Becker *et al.*, 1988;Legendre, 2001;Malosio *et al.*, 1991) and *in vitro* (Tapia and Aguayo, 1998;Withers and St John, 1997), α2 homomers being progressively replaced by α1β heteromers.

To document and quantify the switch in GlyR subtypes occurring during the maturation of spinal cord neurons in our culture system, we analyzed the single-channel conductance of GlyRs in outside-out patches excised from both 2-3 DIV and 11-14 DIV spinal neurons. Indeed, GlyRs are known to exhibit multiple conductance states, ranging from 20 pS to 110 pS, depending on their subunit combination (Bormann *et al.*, 1993). Briefly, α homomeric GlyR are able to open in the whole range of conductance states with a main conductance between 90 and 110 pS whereas the maximal and main conductance state exhibited by αβ heteromeric GlyRs is close to 50 pS (Bormann et al., 1993).

The all-point amplitude histogram of GlyR unitary currents recorded in outside-out patches excised from < 4 DIV spinal neurons (**figure 2B** ; n=9) shows three distinct peaks at 84, 64 and 43 pS. The 84 pS level is the most frequently observed and represent 58 % of the total

Molecular Pharmacology Fast Forward. Published on February 18, 2005 as DOI: 10.1124/mol.104.007435
This article has not been copyedited and formatted. The final version may differ from this version.

open time whereas the 64 pS level and the 43 pS level respectively represent 9 and 33 % of the total open time. In contrast, the all-point amplitude histogram of GlyR unitary currents observed in > 7 DIV spinal neurons (**figure 2D** ; n=8) exhibits only one peak at 38 pS. These results show that young (< 4 DIV) or 'immature' spinal neurons predominantly express α homomeric GlyRs (> 55 pS) which seem to be completely replaced by αβ heteromeric GlyRs in older (> 7 DIV) or 'mature' neurons.

<< Figure 2 should be placed here >>

In the whole-cell configuration of the patch-clamp technique and in voltage-clamp mode at a holding potential of -70 mV, we then analyzed the changes occurring in GlyR pharmacology during this maturation process. It has already been demonstrated that, when maturing *in vitro*, spinal cord neuron GlyRs loose their ability to be modulated by picrotoxin (Tapia and Aguayo, 1998). We, hence, used picrotoxin sensitivity as a tool to discriminate between GlyR homomers and heteromers. **Figure 3A** shows that while 10 µM picrotoxin blocks ~50 % of glycine currents in 2-3 DIV neurons, it only slightly affects the response of 8-15 DIV neurons. This was confirmed by the highly significant difference in picrotoxin concentration-response effect between the two maturation stages (**figure 3B**; $P < 0.001$, ANOVA-2). As shown in **figures 3C** and **3D**, this change in GlyR pharmacology seems also valid for βCCB inhibition. Indeed, the maximal inhibition by 100 µM βCCB dropped from 40.9 ± 5.8 % of control (n = 11) in < 4 DIV spinal cord neurons down to 88.4 ± 4.0 % of control (n = 4) in > 7 DIV neurons ($P < 0.001$, ANOVA-2).

Molecular Pharmacology Fast Forward. Published on February 18, 2005 as DOI: 10.1124/mol.104.007435
This article has not been copyedited and formatted. The final version may differ from this version.

<< Figure 3 should be placed here >>

To further determine if the loss in βCCB sensitivity of spinal cord neuron GlyRs can be related to a switch in GlyR subunit expression, we thus investigated GlyR subunit expression in 'immature' and 'mature' cultures. As seen in **figure 3E**, both α1 and α2 subunit mRNAs are detected by RT-PCR from the beginning of the culture time period while β subunit messengers are only detected in 'mature' neurons. Moreover, quantitative RT-PCR measurements of β subunit transcripts (**figure 3F**) at different culture times show that their appearance coincides with the progressive loss in both picrotoxin and βCCB sensitivity of spinal cord neuron GlyRs. The 4-6 DIV period corresponds to the decaying phase of picrotoxin and βCCB inhibition. Measurements done at this culture maturation stage were thus discarded from all comparisons between 'immature' and 'mature' neurons.

GlyRs of 'immature' hippocampal neurons are also sensitive to β-carbolines

Although it is tempting to conclude from spinal cord neuron experiments that β-carboline inhibition of GlyR is, like picrotoxin inhibition, due to the lack of β subunits in 'immature' cultures, we cannot completely rule out that the reduction in β-carboline sensitivity could also result from the known GlyR α subunit swapping (α2 to α1) described in spinal cord. Therefore, we looked for a neuronal cell type known not to express α1 subunits. Hippocampal neurons could fulfill such a model. Indeed, functional GlyRs have been described in the hippocampus *in vitro* as well as *in vivo* (Mori *et al.*, 2002;Chattipakorn and McMahon, 2002), both during development and in the adulthood (Malosio *et al.*, 1991;Hogg *et al.*, 2004). Their role therein, especially for

Molecular Pharmacology Fast Forward. Published on February 18, 2005 as DOI: 10.1124/mol.104.007435
This article has not been copyedited and formatted. The final version may differ from this version.

what concerns their implication in neurotransmission, remains a matter of debate (Chattipakorn and McMahon, 2002;Mori *et al.*, 2002). Nevertheless, it is well established that they lack α1 subunit expression (Malosio *et al.*, 1991). Indeed, RT-PCR amplification of mRNAs extracted from cultured hippocampal neurons yielded no signal for α1 transcripts (see **figure 5E**).

In order to document a possible functional switch in GlyR subtype in hippocampal neuronal cultures, we first analyzed the single-channel conductance of GlyRs in outside-out patches excised from both 2-3 DIV and 11-14 DIV hippocampal neurons (**figure 4**). The all-point amplitude histogram of GlyR unitary currents recorded in outside-out patches excised from < 4 DIV hippocampal neurons (**figure 4B**; n = 9) shows three peaks at 96, 66 and 45 pS. The 96 pS level is the most frequently observed and represents 48 % of the total open time, whereas the 66 pS and 45 pS levels represent 24 and 33 % of the total open time, respectively. In > 7 DIV hippocampal neurons, the amplitude histogram (**figure 4D**; n = 7) exhibits only two distinct peak at 86 and 45 pS, the 45 pS level being predominant with 77 % of the total open time. As observed in immature spinal neurons, these results show that 'immature' hippocampal neurons functionally express a majority of α homomeric GlyRs (> 55 pS) which are replaced by αβ heteromeric GlyRs in 'mature' hippocampal neurons. Nevertheless, contrasting with mature spinal neurons, 'mature' hippocampal neurons seems to maintain the expression of a small fraction of α homomeric GlyRs.

<< Figure 4 should be placed here >>

In the whole cell recording mode, the inhibition both by β-carbolines and by picrotoxin decreased when hippocampal neurons got older in culture (**figures 5A** to **5D**). For picrotoxin (**figures 5A** and **5B**), the IC_{50} was 0.37 ± 0.05 µM and the maximal inhibition was

Molecular Pharmacology Fast Forward. Published on February 18, 2005 as DOI: 10.1124/mol.104.007435
This article has not been copyedited and formatted. The final version may differ from this version.

12.6 ± 1.7 % of control (n = 4-7) at 2-3 DIV and changed to 2.40 ± 0.44 µM and 22.1 ± 3.9 % of control (n = 4-13) at 10-17 DIV ($P < 0.001$; ANOVA-2). For β-carbolines also, we observed a change with culture age in their blocking property of GlyRs. In the case of βCCB (**figures 5C** and **5D**), the IC_{50} and the maximal inhibition were 0.8 ± 0.2 µM and 39.7 ± 8.0 % of control (n = 5-16) at < 4 DIV and 2.3 ± 1.6 µM and 73.2 ± 3.3 % of control (n = 4-11) at > 7 DIV, respectively ($P < 0.001$; ANOVA-2). A similar shift was obtained with DMCM (data not shown) for which the IC_{50} and the maximal inhibition were 2.8 ± 1.4 µM and 53.1 ± 7.1 % of control (n = 4-33) at < 4 DIV and 0.9 ± 0.9 µM and 83.2 ± 3.5 % of control (n = 5-9) at > 7 DIV, respectively ($P < 0.001$; ANOVA-2).

<< Figure 5 should be placed here >>

RT-PCR amplification of GlyR subunit mRNAs from cultured hippocampal neurons (**figure 5E**) showed that while no α1 is expressed whatever the culture time period, both 'immature' and 'mature' hippocampal neurons express α2, α3 and β subunit transcripts. In spite of the fact that the single-channel recordings and the picrotoxin sensitivity clearly demonstrate an increase in the heteromeric/homomeric GlyRs between < 4 DIV and > 7 DIV, we thus cannot exclude that the decrease in β-carboline sensitivity of GlyRs could be due to an increase in the α3 subunit expression level in hippocampal neurons (see **figure 5E**).

Molecular Pharmacology Fast Forward. Published on February 18, 2005 as DOI: 10.1124/mol.104.007435
This article has not been copyedited and formatted. The final version may differ from this version.

Characterization of α2 homomeric and α2β heteromeric GlyRs stably expressed in CHO cells

To determine if the decrease in β-carboline sensitivity of GlyRs in cultured spinal cord and hippocampal neurons could mainly be due, as known for picrotoxin, to an increase in GlyR β subunit expression, the effects of β-carbolines on glycine-evoked currents were analyzed on CHO cells permanently transfected either with the GlyR α2 subunit alone or in combination with the β subunit.

The quality of the transfection was checked in cloned cells by several experimental approaches. Firstly, total RNA extracted from wild-type, GlyR-α2 and GlyR-α2+β CHO cultures were reverse-transcribed and amplified with primers specific for α2 and β (see **table 1**). This procedure disclosed signals for α2 in the two sets of transfected cells and a signal for β in GlyR-α2+β CHO cultures only (**figure 6A**). Corresponding signals were never found in wild-type CHO cells (**figure 6A**). Secondly, CHO cultures were labeled with anti-GlyR mAb4a antibodies that revealed that GlyRs were expressed at the protein level in transfected cells (**figure 6B**) while absent from wild-type CHO cells (data not shown). Thirdly, the presence of functional GlyRs was assessed by whole-cell patch-clamp electrophysiological recordings. **Figure 6C** illustrates typical responses elicited by 1 mM glycine in cultured wild-type, GlyR-α2 and GlyR-α2+β CHO cells. Glycine responses of recombinant CHO cells were reversibly inhibited by strychnine (data not shown). The glycine EC_{50} and Hill coefficient of glycine-evoked response was 199 ± 31 µM and 1.8 in GlyR-α2 CHO cells (n = 7) and 62.3 ± 10.6 µM and 1.8 in GlyR-α2+β CHO cells (n = 4).

<< Figure 6 should be placed here >>

Molecular Pharmacology Fast Forward. Published on February 18, 2005 as DOI: 10.1124/mol.104.007435
This article has not been copyedited and formatted. The final version may differ from this version.

Functional properties of GlyR subtypes expressed in GlyR-α2 and GlyR-α2+β CHO cells were then studied at the single-channel level in outside-out patches excised from both cell lineages. In this model, true comparisons are allowed because the cell clones have been sequentially generated, *i.e.* the β subunit has been transfected in GlyR-α2 clones, what thus overcome the classical problem of the variable degree of expression (of α2 subunits in this case) when such a process is done in parallel. At -50 mV and with equimolar intra- and extra-cellular Cl^- concentrations, unitary currents evoked by glycine in GlyR-α2 and GlyR-α2+β CHO cells exhibited multiple conductance levels (**figure 7A**). In GlyR-α2 CHO cells, the all-point amplitude histogram of GlyR unitary currents exhibited four conductance peaks at 106, 92, 62 and 45 pS (**figure 7B**). The 106 and 92 pS levels were most frequently observed and represent 36 % and 52 % of the total open time (**figure 7B**, n = 11), respectively. In GlyR-α2+β CHO cells (**figure 7C**, n = 13), the relative proportion of the various conductance levels was greatly modified: the two lowest conductance levels detected at 54 pS (36 % of the total open time) and 22 pS level (24 %) became predominant upon the higher conductance levels detected at 103 pS (23 %) and 92 pS (17%).

The increase in the relative occurrence of the low conductance levels (<55 pS) from 12 to 60 % between GlyR-α2 and GlyR-α2+β CHO cells confirms the expression of functional α2β heteromeric GlyR in the latter cell lineage. Nevertheless, the presence of higher conductance levels (> 55 pS) in GlyR-α2+β CHO cells suggested the persistence of a α2 homomeric GlyR expression.

<< Figure 7 should be placed here >>

Molecular Pharmacology Fast Forward. Published on February 18, 2005 as DOI: 10.1124/mol.104.007435
This article has not been copyedited and formatted. The final version may differ from this version.

Picrotoxin and β-carboline sensitivity of recombinant GlyRs

The relative proportion of high conductance levels (> 55 pS) between GlyR-α2 and GlyR-α2+β CHO cells suggests that ~50 % of the GlyRs expressed by GlyR-α2+β CHO cells are heteromeric. This was confirmed by whole-cell patch-clamp measurements of the inhibition by picrotoxin of glycine-gated currents in both cell types (**figure 8A**). The concentration-response curves of picrotoxin inhibition (**figure 8B**) both differ in their IC_{50} (0.8 ± 0.1 µM, n = 3-47, for GlyR-α2 and 1.6 ± 0.4 µM, n = 8-76, for GlyR-α2+β; $P < 0.001$, ANOVA-2) and their maximal measured inhibition at 100 µM (5.7 ± 1.1 % of control, n = 36, for GlyR-α2 compared to 21.2 ± 2.3 % of control, n = 76, for GlyR-α2+β).

<< Figure 8 should be placed here >>

Then, the effects of βCCB on the glycine responses of both transfected CHO cells were assessed. **Figures 8C** and **8D** demonstrate the highly significant difference in βCCB-induced inhibition between GlyR-α2 and GlyR-α2+β CHO cells. The former had a βCCB IC_{50} of 0.9 ± 0.2 µM and a maximal blocking effect of 43.9 ± 3.0 % of control (n = 6-12) and the latter an IC_{50} of 0.3 ± 0.3 µM and a maximal inhibition of 80.5 ± 4.5 % of control (n = 7-28; $P < 0.001$, ANOVA-2).

Finally, the question arose to know with which site on the GlyR βCCB could interact. We first looked for a competition with picrotoxin since βCCB showed a similar developmentally- and GlyR subunit-dependent effect. Therefore, we measured the inhibitions of glycine-gated currents by 10 µM βCCB and 10 µM picrotoxin alone or in combination on the glycine responses of GlyR-α2 CHO cells. **Figure 8E** demonstrates the additivity of their effects (44.0 ± 6.2 % of

Molecular Pharmacology Fast Forward. Published on February 18, 2005 as DOI: 10.1124/mol.104.007435
This article has not been copyedited and formatted. The final version may differ from this version.

inhibition for βCCB alone compared to 69.3 ± 5.4 % for both compounds together, n = 5; $P < 0.05$, ANOVA-1), hence ruling out that picrotoxin and βCCB share a common site and/or mechanism of inhibition of GlyR function. Second, we checked for the recently described low affinity site for benzodiazepine (Thio *et al.*, 2003) by measuring the interaction of 10 µM βCCB with 10 µM Ro 15-1788 (flumazenil), the prototypic benzodiazepine antagonist at $GABA_A$Rs. As shown in **figure 8F**, flumazenil reversed the inhibition of glycine currents by βCCB to control level (9.6 ± 0.7 % of inhibition with both drugs compared to 29.6 ± 2.9 % for βCCB alone, n = 8; $P < 0.001$, ANOVA-1).

Molecular Pharmacology Fast Forward. Published on February 18, 2005 as DOI: 10.1124/mol.104.007435
This article has not been copyedited and formatted. The final version may differ from this version.

Discussion

In this work, we have shown that β-carboline inhibition is only observed in 'immature' (< 4 DIV) cultured spinal cord and hippocampal neurons, predominantly expressing α homomeric GlyRs. 'Mature' (> 7 DIV) neuron insensitivity to β-carbolines paralleled their insensitivity to picrotoxin and was correlated with the replacement of α homomeric by αβ heteromeric GlyRs in both cell type. We definitely conclude that the expression of β subunits is sufficient to account for the disappearance of β-carboline inhibition by comparing the pharmacological profiles of CHO cells stably transfected with GlyR-α2 and GlyR-α2+β subunits. We also report, for the first time, that cultured hippocampal neurons undergo, like spinal cord neurons, a developmental regulation of their GlyR properties during *in vitro* maturation.

β-carbolines are antagonists of α_2 homomeric GlyRs

Pharmacological agents have been invaluable tools to study ion channel function. Available drugs that could help us studying strychnine-sensitive GlyRs are however much less abundant than for example for $GABA_A$Rs (Laube, 2002). So far, picrotoxin (Lynch *et al.*, 1995), and more recently some quinoxalines (Meier and Schmieden, 2003), are the only known pharmacological tools able to discriminate between homomeric and heteromeric GlyRs. Here, we report that β-carbolines, which are known benzodiazepine inverse agonists at $GABA_A$Rs, can also fulfill such a role. In spinal neurons, the amount of blockade induced by the two inhibitors remains very close and both of them easily discriminate between 'immature' and 'mature' spinal GlyRs. By contrast, in hippocampal neurons and transfected CHO cells, βC seems to be a better tool than picrotoxin to detect the partial homomer/heteromer switch observed in these cells.

Molecular Pharmacology Fast Forward. Published on February 18, 2005 as DOI: 10.1124/mol.104.007435
This article has not been copyedited and formatted. The final version may differ from this version.

Indeed, in the case of picrotoxin, we mainly observed a slight shift in the IC_{50} whereas both IC_{50} and maximal inhibition were affected in the case of βCs. Therefore, a complete concentration-inhibition curve should be needed to document the switch with picrotoxin, whereas a single inhibition assay at a high β-carboline concentration (> 10 μM) would be sufficient to estimate the ratio homomer/heteromer.

In our models, picrotoxin inhibition of GlyRs paralleled that of β-carbolines, raising the question of a common binding site on α2 homomeric GlyRs. This is however very unlikely since the inhibitions by β-carbolines and picrotoxin are additive. Concerning the putative GlyR binding site for β-carbolines, when we first reported β-carboline inhibition of GlyRs in 'immature' cultured spinal cord neurons and its reversal by some antiepileptic drugs (Rigo *et al.*, 2002), we already suggested that it could be mediated by a low affinity benzodiazepine site common to GlyR and $GABA_AR$, already previously described in the latter (Walters *et al.*, 2000). This hypothesis was recently reinforced by the finding that some benzodiazepines inhibit glycine responses of α2-containing GlyRs from cultured hippocampal neurons (Thio *et al.*, 2003). Our observed reversal of β-carboline inhibition by flumazenil, a benzodiazepine antagonist at $GABA_ARs$, further supports this hypothesis.

In vitro maturation of GlyRs in spinal cord and hippocampal neurons

Supporter by morphological as well as functional argument, several reports have already documented the developmental switch in GlyR subunit expression (embryonic-neonatal α2 homomers – juvenile α2β heteromers – adult α1β heteromers) underlying the change in glycinergic transmission that occurs, both *in vitro* and *in vivo*, in spinal cord and brainstem neurons (Singer and Berger, 2000;Singer *et al.*, 1998;Tapia and Aguayo, 1998;Withers and St

Molecular Pharmacology Fast Forward. Published on February 18, 2005 as DOI: 10.1124/mol.104.007435
This article has not been copyedited and formatted. The final version may differ from this version.

John, 1997). Here, combining quantitative RT-PCR and single-channel recordings, we further characterize this developmental schedule by showing that the appearance of functional αβ heteromers during the *in vitro* maturation of spinal cord neurons is at least in part due to a transcriptional regulation of the β subunit expression.

As already mentioned in the introduction, GlyRs are also known to be expressed in more rostral regions of the CNS. The exact subunit composition of the GlyRs expressed in those regions is poorly documented and, so far, no true developmental regulation, as the one that occurs in the spinal cord, has been described. Our study clearly shows that GlyRs expressed by hippocampal neurons undergo such a developmental regulation during *in vitro* maturation. However, this maturation process differs from spinal neurons in several aspects. Firstly, the persistence of high conductance levels in 11-14 DIV hippocampal neurons show that the replacement of homomers by heteromers is not complete at this time. Such a persistence of homomeric GlyRs is also supported by the higher β-carboline and picrotoxin sensitivity of glycine-evoked currents in 'mature' hippocampal neurons compared to 'mature' spinal neurons. This observation could result from a slower maturation process in hippocampal neurons. However, homomeric GlyRs are known to be expressed by 'mature' hippocampal neurons recorded in 4-week-old rat brain slices, supporting the hypothesis of a 'partial' maturation process in hippocampal neurons (Chattipakorn & McMahon, 2002).

RT-PCR experiments show that no qualitative change of GlyR subunits occurred during the *in vitro* maturation of hippocampal neurons: at least at the transcript level, α2, α3 and β subunits were present from the beginning of the culture period. Although no α2-to-α1 subunit switch occurs in hippocampal neurons, one can hypothesize an alternative α2-to-α3 switch. However, we observed very similar pharmacological properties between < 4 DIV hippocampal

Molecular Pharmacology Fast Forward. Published on February 18, 2005 as DOI: 10.1124/mol.104.007435
This article has not been copyedited and formatted. The final version may differ from this version.

neurons and GlyR-α2 CHO cells on the one hand and between > 7 DIV hippocampal neurons and GlyR-α2+β CHO cells on the other hand. Since the ratio of high (> 55 pS) *vs* low (< 55 pS) conductance levels is similar in both case, we can speculate that either α2-contaning GlyRs have the same pharmacological properties than α3-containing GlyRs or that the α3 subunit is poorly expressed in hippocampal neurons. The latter hypothesis could explain the fact that Thio et al. were unable to detect α3 subunit transcript in 4-14 DIV hippocampal neurons (Thio et al., 2003).

Pathophysiological and physiological implications

A still unresolved question concerns the actual existence of endogenous allosteric modulators of ligand-gated channels. In that respect, and regarding inhibitory receptors, almost only zinc (Suwa *et al.*, 2001;Barberis *et al.*, 2000) and protons (Chen *et al.*, 2004) were conclusively demonstrated as endogenous modulators. Some β-carbolines, *e.g.* βCCB used in this study, were also proposed as endogenous compounds, but this has not been studied further for more than ten years (Medina *et al.*, 1989;Braestrup *et al.*, 1980). To what extent these modulators actually influence neurotransmission or other inhibitory receptor-mediated effects remains largely unknown.

Extrasynaptic homomeric α2-containing GlyRs have been described in the adult brain where they have been proposed to participate in the tonic regulation of excitability (Mori *et al.*, 2002;Chattipakorn and McMahon, 2003), hence being interesting targets for excitability disorders, such a epilepsy. In that respect, it has been demonstrated that some antiepileptic drugs, *e.g.* levetiracetam, are able to reverse both β-carboline- and zinc-induced inhibition not only of $GABA_A$Rs but also of GlyRs (Rigo *et al.*, 2002). GlyRs have also been proposed to participate in developmental processes (Flint *et al.*, 1998) and, more recently, α2-containing GlyRs have even

Molecular Pharmacology Fast Forward. Published on February 18, 2005 as DOI: 10.1124/mol.104.007435
This article has not been copyedited and formatted. The final version may differ from this version.

been described in progenitors of rod photoreceptor in the retina (Young and Cepko, 2004). Hence, further characterizing the properties and the roles of ‘immature’ GlyRs certainly deserves further attention.

Molecular Pharmacology Fast Forward. Published on February 18, 2005 as DOI: 10.1124/mol.104.007435
This article has not been copyedited and formatted. The final version may differ from this version.

Acknowledgments

We thank P. Ernst-Gengoux, A. Brose, P. Coucke and C. Mazy-Servais for their technical support and expertise. G. Hans, S. Belachew and B. Rogister are respectively Research Fellow, Research Associate and Senior Research Associate of the FNRS.

Molecular Pharmacology Fast Forward. Published on February 18, 2005 as DOI: 10.1124/mol.104.007435
This article has not been copyedited and formatted. The final version may differ from this version.

References

Barberis A, Cherubini E and Mozrzymas J W (2000) Zinc Inhibits Miniature GABAergic Currents by Allosteric Modulation of GABAA Receptor Gating. *J Neurosci* **20**: pp 8618-8627.

Beato M, Groot-Kormelink P J, Colquhoun D and Sivilotti L G (2004) The Activation Mechanism of Alpha1 Homomeric Glycine Receptors. *J Neurosci* **24**: pp 895-906.

Becker CM, Hoch W and Betz H (1988) Glycine Receptor Heterogeneity in Rat Spinal Cord During Postnatal Development. *EMBO J* **7**: pp 3717-3726.

Bormann J, Rundstrom N, Betz H and Langosch D (1993) Residues Within Transmembrane Segment M2 Determine Chloride Conductance of Glycine Receptor Homo- and Hetero-Oligomers. *EMBO J* **12**: pp 3729-3737.

Braestrup C, Nielsen M and Olsen C E (1980) Urinary and Brain B-Carboline-3-Carboxylates As Potent Inhibitors of Brain Benzodiazepine Receptors. *Proc Natl Acad Sci USA* **77**: pp 2288-2292.

Chattipakorn SC and McMahon L L (2002) Pharmacological Characterization of Glycine-Gated Chloride Currents Recorded in Rat Hippocampal Slices. *J Neurophysiol* **87**: pp 1515-1525.

Chattipakorn SC and McMahon L L (2003) Strychnine-Sensitive Glycine Receptors Depress Hyperexcitability in Rat Dentate Gyrus. *J Neurophysiol* **89**: pp 1339-1342.

Chen Z, Dillon G H and Huang R (2004) Molecular Determinants of Proton Modulation of Glycine Receptors. *J Biol Chem* **279**: pp 876-883.

Flint AC, Liu X and Kriegstein A R (1998) Nonsynaptic Glycine Receptor Activation During Early Neocortical Development. *Neuron* **20**: pp 43-53.

Hogg RC, Chipperfield H, Whyte K A, Stafford M R, Hansen M A, Cool S M, Nurcombe V and Adams D J (2004) Functional Maturation of Isolated Neural Progenitor Cells From the Adult Rat Hippocampus. *Eur J Neurosci* **19**: pp 2410-2420.

Laube B (2002) Potentiation of Inhibitory Glycinergic Neurotransmission by Zn2+: a Synergistic Interplay Between Presynaptic P2X2 and Postsynaptic Glycine Receptors. *Eur J Neurosci* **16**: pp 1025-1036.

Laube B, Maksay G, Schemm R and Betz H (2002) Modulation of Glycine Receptor Function: a Novel Approach for Therapeutic Intervention at Inhibitory Synapses? *Trends Pharmacol Sci* **23**: pp 519-527.

Legendre P (2001) The Glycinergic Inhibitory Synapse. *Cell Mol Life Sci* **58**: pp 760-793.

Leprince P, Lefebvre P P, Rigo J-M, Delrée P, Rogister B and Moonen G (1989) Cultured Astroglia Release a Neuronotoxic Activity That Is Not Related to the Excitotoxins. *Brain Res* **502**: pp 21-27.

Lynch JW, Rajendra S, Barry P H and Schofield P R (1995) Mutations Affecting the Glycine Receptor Agonist Transduction Mechanism Convert the Competitive Antagonist, Picrotoxin, into an Allosteric Potentiator. *J Biol Chem* **270**: pp 13799-13806.

Malosio ML, Marqueze-Pouey B, Kuhse J and Betz H (1991) Widespread Expression of Glycine Receptor Subunit MRNAs in the Adult and Developing Rat Brain. *EMBO J* **10**: pp 2401-2409.

Mangin JM, Baloul M, Prado D C, Rogister B, Rigo J M and Legendre P (2003) Kinetic Properties of the Alpha2 Homo-Oligomeric Glycine Receptor Impairs a Proper Synaptic Functioning. *J Physiol* **553**: pp 369-386.

Mangin JM, Guyon A, Eugene D, Paupardin-Tritsch D and Legendre P (2002) Functional Glycine Receptor Maturation in the Absence of Glycinergic Input in Dopaminergic Neurones of the Rat Substantia Nigra. *J Physiol* **542**: pp 685-697.

McCool BA and Farroni J S (2001) Subunit Composition of Strychnine-Sensitive Glycine Receptors Expressed by Adult Rat Basolateral Amygdala Neurons. *Eur J Neurosci* **14**: pp 1082-1090.

Medina JH, de Stein M L and De Robertis E (1989) N-[3H]Butyl-Beta-Carboline-3-Carboxylate, a Putative Endogenous Ligand, Binds Preferentially to Subtype 1 of Central Benzodiazepine Receptors. *J Neurochem* **52**: pp 665-670.

Meier J and Schmieden V (2003) Inhibition of Alpha-Subunit Glycine Receptors by Quinoxalines. *Neuroreport* **14**: pp 1507-1510.

Mori M, Gahwiler B H and Gerber U (2002) Beta-Alanine and Taurine As Endogenous Agonists at Glycine Receptors in Rat Hippocampus in Vitro. *J Physiol* **539**: pp 191-200.

Moss SJ and Smart T G (2001) Constructing Inhibitory Synapses. *Nat Rev Neurosci* **2**: pp 240-250.

Nguyen L, Malgrange B, Belachew S, Rogister B, Rocher V, Moonen G and Rigo J-M (2002) Functional Glycine Receptors Are Expressed by Postnatal Nestin Positive Neural Stem/Progenitor Cells. *Eur J Neurosci* **15**: pp 1299-1305.

Ortells MO and Lunt G G (1995) Evolutionary History of the Ligand-Gated Ion-Channel Superfamily of Receptors. *Trends Neurosci* **18**: pp 121-127.

Rigo JM, Hans G, Nguyen L, Rocher V, Belachew S, Malgrange B, Leprince P, Moonen G, Selak I, Matagne A and Klitgaard H (2002) The Anti-Epileptic Drug Levetiracetam Reverses the Inhibition by Negative Allosteric Modulators of Neuronal. *Br J Pharmacol* **136**: pp 659-672.

Rigo, J.-M., Coucke, P., Rogister, B., Belachew, S., Mazy-Servais, C., and Moonen, G. β-carbolines: negative allosteric modulators of GABA- and glycine-gated chloride channels. Society for Neuroscience Meeting , 1759. 1998.

Schrader N, Kim E Y, Winking J, Paulukat J, Schindelin H and Schwarz G (2004) Biochemical Characterization of the High Affinity Binding Between the Glycine Receptor and Gephyrin. *J Biol Chem*.

Sergeeva OA and Haas H L (2001) Expression and Function of Glycine Receptors in Striatal Cholinergic Interneurons From Rat and Mouse. *Neuroscience* **104**: pp 1043-1055.

Singer JH and Berger A J (2000) Development of Inhibitory Synaptic Transmission to Motoneurons. *Brain Res Bull* **53**: pp 553-560.

Singer JH, Talley E M, Bayliss D A and Berger A J (1998) Development of Glycinergic Synaptic Transmission to Rat Brain Stem Motoneurons. *J Neurophysiol* **80**: pp 2608-2620.

Suwa H, Saint-Amant L, Triller A, Drapeau P and Legendre P (2001) High-Affinity Zinc Potentiation of Inhibitory Postsynaptic Glycinergic Currents in the Zebrafish Hindbrain. *J Neurophysiol* **85**: pp 912-925.

Tapia JC and Aguayo L G (1998) Changes in the Properties of Developing Glycine Receptors in Cultured Mouse Spinal Neurons. *Synapse* **28**: pp 185-194.

Teuber L, Watjens F and Jensen L H (1999) Ligands for the Benzodiazepine Binding Site--a Survey. *Curr Pharm Des* **5**: pp 317-343.

Thio LL, Shanmugam A, Isenberg K and Yamada K (2003) Benzodiazepines Block Alpha2-Containing Inhibitory Glycine Receptors in Embryonic Mouse Hippocampal Neurons. *J Neurophysiol* **90**: pp 89-99.

Virginio C and Cherubini E (1997) Glycine-Activated Whole Cell and Single Channel Currents in Rat Cerebellar Granule Cells in Culture. *Brain Res Dev Brain Res* **98**: pp 30-40.

Walters RJ, Hadley S H, Morris K D and Amin J (2000) Benzodiazepines Act on GABAA Receptors Via Two Distinct and Separable Mechanisms. *Nat Neurosci* **3**: pp 1274-1281.

Withers MD and St John P A (1997) Embryonic Rat Spinal Cord Neurons Change Expression of Glycine Receptor Subtypes During Development *in Vitro*. *J Neurobiol* **32**: pp 579-592.

Ye J (2000) Physiology and Pharmacology of Native Glycine Receptors in Developing Rat Ventral Tegmental Area Neurons. *Brain Res* **862**: pp 74-82.

Young TL and Cepko C L (2004) A Role for Ligand-Gated Ion Channels in Rod Photoreceptor Development. *Neuron* **41**: pp 867-879.

Molecular Pharmacology Fast Forward. Published on February 18, 2005 as DOI: 10.1124/mol.104.007435
This article has not been copyedited and formatted. The final version may differ from this version.

Footnotes

£ This work was supported by the *Fonds pour la Formation à la Recherche dans l'Industrie et dans l'Agriculture* (FRIA, Belgium), the *Fonds National de la Recherche Scientifique* (FNRS, Belgium), the *Fondation Médicale Reine Elisabeth* (FMRE, Belgium), the *Ligue belge pour la sclérose en plaque* (Belgium), INSERM (France), the *Fondation pour la Recherche Médicale* (FRM, France), the *Centre National de la Recherche Scientifique* (CNRS, France) and INSERM - CFB agreement (P. Legendre and J.M. Rigo).

* J.-M.M., L.N., P.L. and J.-M.R. contributed equally to this work

Center for Cellular and Molecular Neuroscience, University of Liège, 17 place Delcour, B-4020 Liège, Belgium (J.-M.M., L.N., C.G., G.H., B.R., S.B., G.M., J.-M.R.); Department of Neurology, University of Liège, CHU Sart-Tilman B35, B-4000 Liège, Belgium (B.R., S.B., G.M.); UMR 7102 CNRS, Université Pierre et Marie Curie, Bât B 6ème étage, 7 Quai Saint Bernard, 75252 Paris Cedex 05, France (J.-M.M., P.L.); Division of Molecular Neurobiology, National Institute for Medical Research, The Ridgeway, Mill Hill, London, NW7 IAA (L.N.); Department of Physiology, Transnationale Universiteit Limburg / Limburgs Universitair Centrum, Biomedisch Onderzoekinstituut, B-3590 Diepenbeek, Belgium (J.-M.R.)

Molecular Pharmacology Fast Forward. Published on February 18, 2005 as DOI: 10.1124/mol.104.007435
This article has not been copyedited and formatted. The final version may differ from this version.

Legends for Figures

Figure 1 – β-carbolines reversibly inhibit glycine-induced currents in cultured spinal cord neurons

A-B The same 3-day-*in vitro* (3 DIV) spinal cord neuron was voltage-clamped at a holding potential of -70 mV using the whole-cell patch-clamp technique (see methods) and currents induced by a 10 s perfusion of 50 µM GABA (**A**) or a 15 s perfusion of 100 µM glycine (**B**) alone or in combination with 100 µM βCCB were recorded. βCCB was perfused for 15 s before being co-applied with agonists. A 60 s period was allowed for the washout of drugs.

C Currents evoked by 100 µM glycine in 2-3 DIV spinal cord neurons were recorded in the presence of increasing βCCB (black filled circles), DMCM (gray filled circles) and FG7142 (empty circles) concentrations. Results are expressed as percentage of glycine-induced currents peak amplitudes in the absence of β-carbolines (mean ± SEM, n = 3-15 for βCCB, 3-26 for DMCM and 4-8 for FG7142).

Figure 2 – Distinct repartition of GlyR conductance levels between immature and mature spinal cord neurons

A,C Examples of unitary currents evoked by application of 100 µM glycine on outside-out patches excised from 2-3 DIV (**A**) and 11-14 DIV (**C**) spinal neurons (holding potential = -50mV). The closed state C is marked by a continuous line. Conductance levels detected in the all-point histograms shown in **B** and **D** are indicated by dotted line and labeled from the lowest conductance level O1 to the highest O3. Traces were sampled at 20 kHz and

Molecular Pharmacology Fast Forward. Published on February 18, 2005 as DOI: 10.1124/mol.104.007435
This article has not been copyedited and formatted. The final version may differ from this version.

filtered at 2 kHz, and correspond to epochs from longer recordings obtained from different patches.

B,D Point-per-point amplitude histograms of unitary currents evoked by 100 µM of glycine applied on outside-out patches excised from 2-3 DIV (**B**) and 11-14 DIV (**D**) spinal neurons. The amplitude histogram was obtained by pooling recorded epochs of 25-50 s from 9 (**B**) and 8 (**D**) patches. The amplitude histogram was best fitted by the sum of three (**B**) or by only one (**D**) Gaussian functions. The mean conductances and the relative areas are indicated for each Gaussian function. The conductance was determined from the mean amplitude of each Gaussian function with E_{Cl} = -2mV (holding potential = -50 mV). The amplitude histograms were normalized using the current amplitude distribution corresponding to the baseline. The bin width is 0.05 pA.

Figure 3 – Spinal cord neuron GlyR subunit composition and pharmacology are culture time-dependent

A,C 2-3 (< *4 DIV*) and 8-15 (> *7 DIV*) DIV spinal cord neurons were perfused for 10 s with 100 µM glycine alone or in combination with 10 µM picrotoxin (PIC, **A**) or 10 µM βCCB (**C**). A 15 s pre-treatment of the drugs was done and a 60 s period was allowed for the washout of the drugs.

B,D Currents elicited by 100 µM glycine in < *4 DIV* and in > *7 DIV* spinal cord neurons were recorded for increasing picrotoxin (PIC, **B**) or βCCB (**D**) concentrations. Results are expressed as percentage of glycine-induced currents peak amplitudes in the absence of any drug (mean ± SEM, n = 3-10 for < *4 DIV*, **B**, 3-5 for > *7 DIV*, **B**, 3-15 for < *4 DIV*, **D**, and 4-5 for > *7 DIV*, **D**).

Molecular Pharmacology Fast Forward. Published on February 18, 2005 as DOI: 10.1124/mol.104.007435
This article has not been copyedited and formatted. The final version may differ from this version.

E RT-PCR amplification of GlyR α1, α2 and β subunit transcripts in total RNA extracted from 2-3 (*< 4 DIV*) and 8-15 (*> 7 DIV*) DIV cultured spinal cord neurons and adult mouse brain tissue (*Ad.*). Signals corresponding to α1 (211 bp), α2 (182 bp) and β (228 bp) were detected (+, with RT; –, negative controls without RT in order to exclude a possible genomic DNA contamination of RNA preparation). Left margins indicate migration of standard DNA markers the size of which is indicated in base pairs.

F Picrotoxin (*PIC*) and βCCB inhibition of glycine-induced currents recorded in spinal cord neurons (*left ordinate axis*) and the level of β subunit transcript expression detected by quantitative RT-PCR (*right ordinate axis*) are expressed as a function of culture time. For glycine-induced currents, results are expressed as 100-percentage of glycine-induced currents peak amplitudes in the absence of any drug (mean ± SEM; n = 10).

Figure 4 – Distinct repartition of GlyR conductance levels between immature and mature hippocampal neurons

A,C Examples of unitary currents evoked by application of 100 µM glycine on outside-out patches excised from 2-3 DIV (**A**) and 11-14 DIV (**C**) hippocampal neurons (holding potential = -50mV). The closed state C is marked by a continuous line. The conductance levels detected in the all-point histogram shown in **B** and **D** are indicated by dotted line and labeled from the lowest conductance level O1 to the highest O3. Traces were sampled at 20 kHz and filtered at 2 kHz, and correspond to epochs from longer recordings obtained from different patches.

B,D Point-per-point amplitude histogram of unitary currents evoked by 100 µM of glycine applied on outside-out patches excised from 2-3 DIV (**B**) and 11-14 DIV (**D**) hippocampal

Molecular Pharmacology Fast Forward. Published on February 18, 2005 as DOI: 10.1124/mol.104.007435
This article has not been copyedited and formatted. The final version may differ from this version.

neurons. The amplitude histogram was obtained by pooling recorded epochs of 25-50 s from 9 (**B**) and 7 (**D**) patches. The amplitude histograms were best fitted by the sum of three (**B**) or two (**D**) Gaussian functions. The mean conductances and the relative areas are indicated for each Gaussian function. The conductance was determined from the mean amplitude of each Gaussian function with E_{Cl} = -2mV (holding potential = -50 mV). The amplitude histogram was normalized using the current amplitude distribution corresponding to the baseline. The bin width is 0.05 pA.

Figure 5 – βCCB and picrotoxin inhibition of glycine-gated currents in cultured hippocampal neurons

A,C 2-3 (*< 4 DIV*) and 10-17 (*> 7 DIV*) DIV hippocampal neurons were perfused for 10 s with 100 µM glycine alone or in combination with 10 µM picrotoxin (PIC, **A**) or 10 µM βCCB (**C**). A 15 s pre-treatment of the drugs was done and a 60 s period was allowed for the washout of the drugs.

B,D Currents elicited by 100 µM glycine in *< 4 DIV* and in *> 7 DIV* hippocampal neurons were recorded for increasing picrotoxin (PIC, **B**) or βCCB (**D**) concentrations. Results are expressed as percentage of glycine-induced currents peak amplitudes in the absence of any drug (mean ± SEM, n = 3-7 for *< 4 DIV*, **B**, 4-13 for *> 7 DIV*, **B**, 5-16 for *< 4 DIV*, **D**, and 4-11 for *> 7 DIV*, **D**).

E RT-PCR amplification of GlyR α1, α2, α3 and β subunit transcripts in total RNA extracted from 2-3 (*< 4 DIV*) and 10-17 (*> 7 DIV*) DIV cultured hippocampal neurons. No signal corresponding to α1 (211 bp), but well signal corresponding to α2 (182 bp), α3 (309 bp) and β (228 bp) were detected (+, with RT; –, negative controls without RT). Left

Molecular Pharmacology Fast Forward. Published on February 18, 2005 as DOI: 10.1124/mol.104.007435
This article has not been copyedited and formatted. The final version may differ from this version.

margins indicate migration of standard DNA markers the size of which is indicated in base pairs.

Figure 6 – Morpho-functional characterization of GlyRs expressed by transfected GlyR-α2 and GlyR-α2+β CHO cells

A RT-PCR amplification of GlyR α2 and β subunit transcripts in total RNA extracted from cultured wild-type (*CHO*), GlyR-α2-transfected (*GlyR-α2*), GlyR-α2+β-transfected (*GlyR-α2+β*) CHO cells and neonate mouse spinal cords (*SC*). Signals corresponding to α2 (182 bp) and β (228 bp) were detected (+, with RT; –, negative controls without RT). Right margins indicate migration of standard DNA markers the size of which is indicated in base pairs.

B Confocal images of GlyR-α2 and GlyR-α2+β CHO cells immunoreactive for GlyR (gray). Scale bar: 20 μm.

C Currents induced by a 15 s application of 1 mM glycine in whole-cell patch-clamped and voltage-clamped (holding potential = -70 mV) wild-type (*CHO*), GlyR-α2-transfected (*GlyR-α2*) and GlyR-α2+β-transfected (*GlyR-α2+β*) CHO cells.

D Concentration response curves of currents evoked by increasing glycine concentrations were recorded in *GlyR-α2* (black dots) and in *GlyR-α2+β* (gray dots) CHO cells. Results are expressed as percentage of currents induced by 1 mM glycine (mean ± SEM, n = 7 for *GlyR-α2* and 4 for *GlyR-α2+β*).

Molecular Pharmacology Fast Forward. Published on February 18, 2005 as DOI: 10.1124/mol.104.007435
This article has not been copyedited and formatted. The final version may differ from this version.

Figure 7 – Distinct repartition of GlyR conductance levels between GlyR-α2 and GlyR-α2+β CHO cells

A Examples of unitary currents evoked by 100 µM glycine applied on outside-out patches excised from *GlyR-α2* or *GlyR-α2+β* CHO (holding potential = -50mV). The closed state C is indicated by a continuous line whereas open states are indicated by a dotted line and labeled from the lowest level O1 to the highest level O5. Traces were sampled at 25 kHz and filtered at 1 kHz, and correspond to epochs from longer recordings obtained from differents patches.

B, C Point-per-point amplitude histograms of unitary currents evoked by 100 µM of glycine applied on outside-out patches excised from *GlyR-α2* (**B**) and *GlyR-α2+β* (**C**) CHO cells. The amplitude histograms shown in **B** and **C** were obtained by pooling recorded epochs of 50 s from 11 and 13 patches, respectively. Amplitude histograms were best fitted by the sum of four Gaussian functions. The mean conductances and the relative areas are indicated for each Gaussian function. Conductance levels were determined from the mean amplitude of each Gaussian function with E_{Cl} = -2mV (holding potential = -50 mV). Amplitude histograms were normalized using the current amplitude distribution corresponding to the baseline. The bin width is 0.1 pA.

Molecular Pharmacology Fast Forward. Published on February 18, 2005 as DOI: 10.1124/mol.104.007435
This article has not been copyedited and formatted. The final version may differ from this version.

Figure 8 – βCCB and picrotoxin sensitivity of GlyR-α2 and GlyR-α2+β CHO cells

A,C *GlyR-α2* and *GlyR-α2+β* CHO cells were perfused for 10 s with 100 µM glycine alone or in combination with 10 µM picrotoxin (PIC, **A**) or 10 µM βCCB (**C**). A 15 s pre-treatment of the drugs was done and a 60 s period was allowed for the washout of the drugs.

B,D Currents elicited by 100 µM glycine in *GlyR-α2* and in *GlyR-α2+β* CHO cells were recorded for increasing picrotoxin (PIC, **B**) or βCCB (**D**) concentrations. Results are expressed as percentage of glycine-induced currents peak amplitudes in the absence of any drug (mean ± SEM, n = 3-47 for *GlyR-α2*, **B**, 5-29 for *GlyR-α2+β*, **B**, 6-17 for *GlyR-α2*, **D**, and 7-28 for *GlyR-α2+β*, **D**).

E Currents elicited by 100 µM glycine in *GlyR-α2* CHO cells were recorded in the presence of either 10 µM βCCB or picrotoxin (*PIC*) alone or in combination. Results are expressed as percentage of glycine-induced currents peak amplitudes in the absence of any drug (mean ± SEM, n = 4-5; * $P < 0.05$, one-way analysis of variance followed by Dunnet's post-tests).

F Currents elicited by 100 µM glycine in 3 DIV spinal cord neurons were recorded in the presence of either 10 µM βCCB or flumazenil (*FLU*) alone or in combination. Results are expressed as percentage of glycine-induced currents peak amplitudes in the absence of any drug (mean ± SEM, n = 6-8; *** $P < 0.001$, one-way analysis of variance followed by Dunnet's post-tests).

Molecular Pharmacology Fast Forward. Published on February 18, 2005 as DOI: 10.1124/mol.104.007435
This article has not been copyedited and formatted. The final version may differ from this version.

Tables and Figures

Table 1 – Sequences of primers (forward, for.; reverse, rev.) used for PCR

cDNA	**Primer**	**Size of product (base pairs)**	**References**
GlyR α1	For. 5'-GTC CCA ACA ACA ACA ACA CC-3' Rev. 5'-TCC CAG AGC CTT CAC TTG TT-3'	211	(Nguyen *et al.*, 2002)
GlyR α2	For. 5'-CTA CAC CTG CCA ACC CAC-3' Rev. 5'-CTT GTG GAC ATC TTC ATG CC-3'	182	(Nguyen *et al.*, 2002)
GlyR α3	For. 5'-GCA CTG GAG AAG TTT TAC CG-3' Rev. 5'-AAT CTT GCT GAT GAT TGA ATG TC-3'	309	(Thio *et al.*, 2003)
GlyR β	For. 5'-GAA GAA CAC TGT GAA CGG CA-3' Rev. 5'-GGC TTC TTG TTC TTT GCC TG-3'	228	(Nguyen *et al.*, 2002)

Molecular Pharmacology Fast Forward. Published on February 18, 2005 as DOI: 10.1124/mol.104.007435
This article has not been copyedited and formatted. The final version may differ from this version.

Figure 1

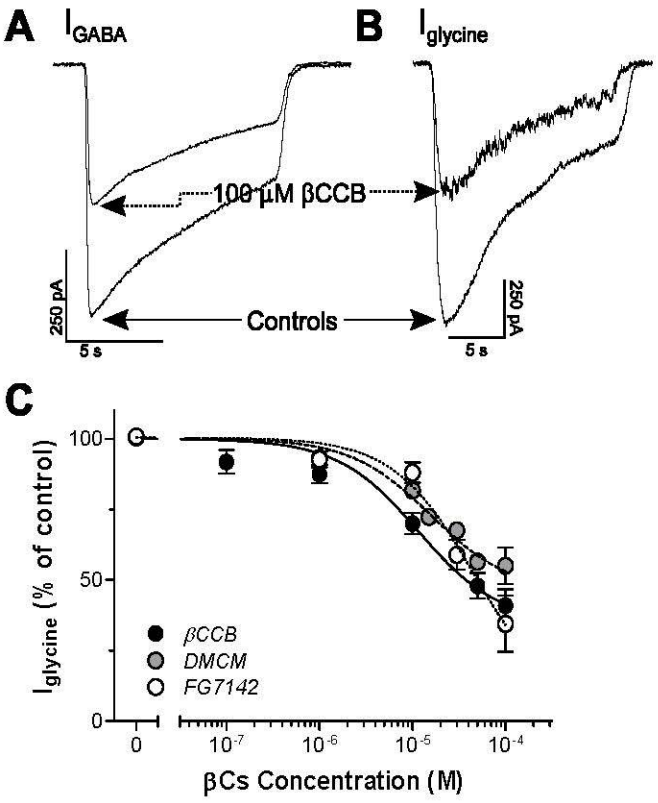

Molecular Pharmacology Fast Forward. Published on February 18, 2005 as DOI: 10.1124/mol.104.007435
This article has not been copyedited and formatted. The final version may differ from this version.

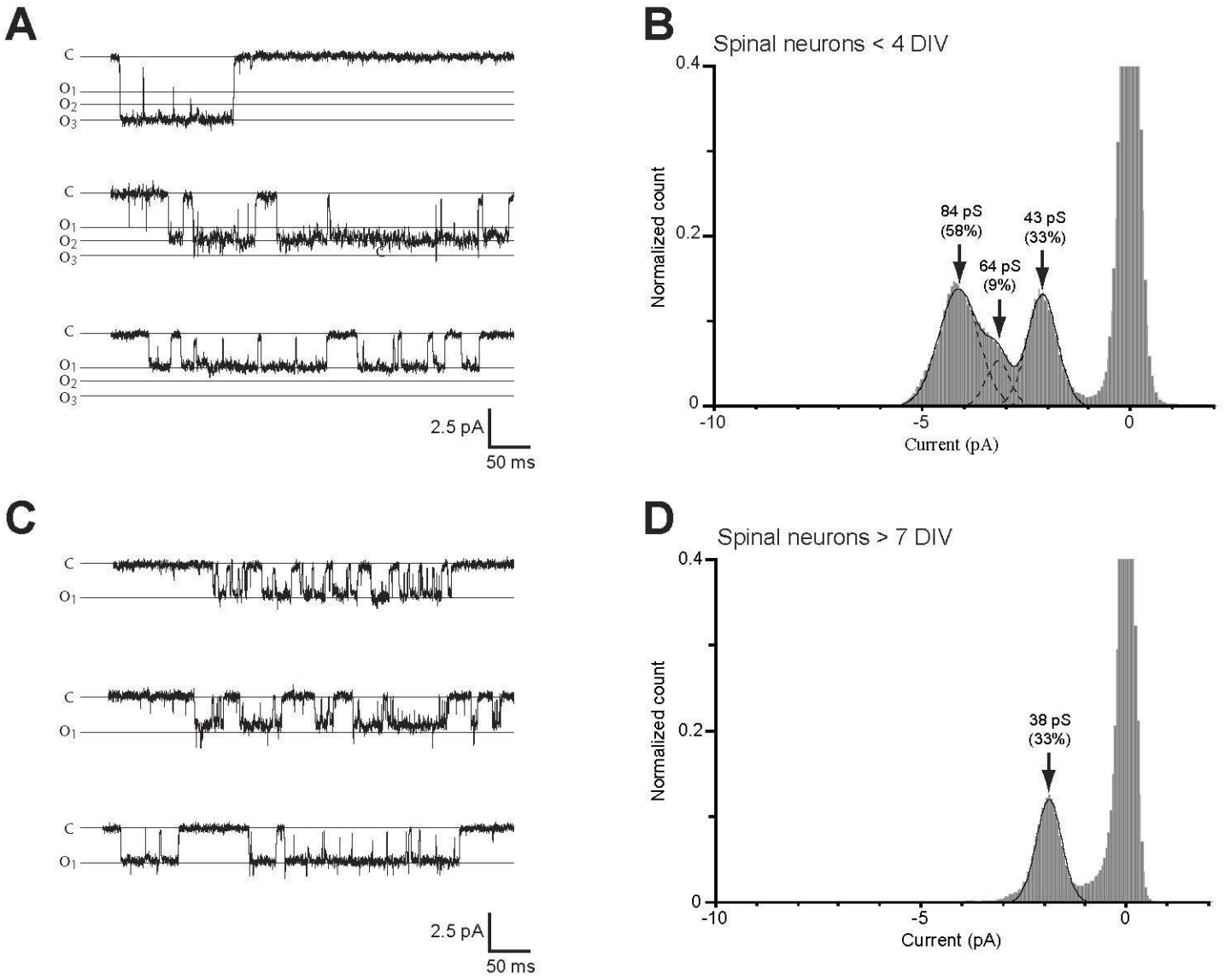

Molecular Pharmacology Fast Forward. Published on February 18, 2005 as DOI: 10.1124/mol.104.007435
This article has not been copyedited and formatted. The final version may differ from this version.

Figure 3

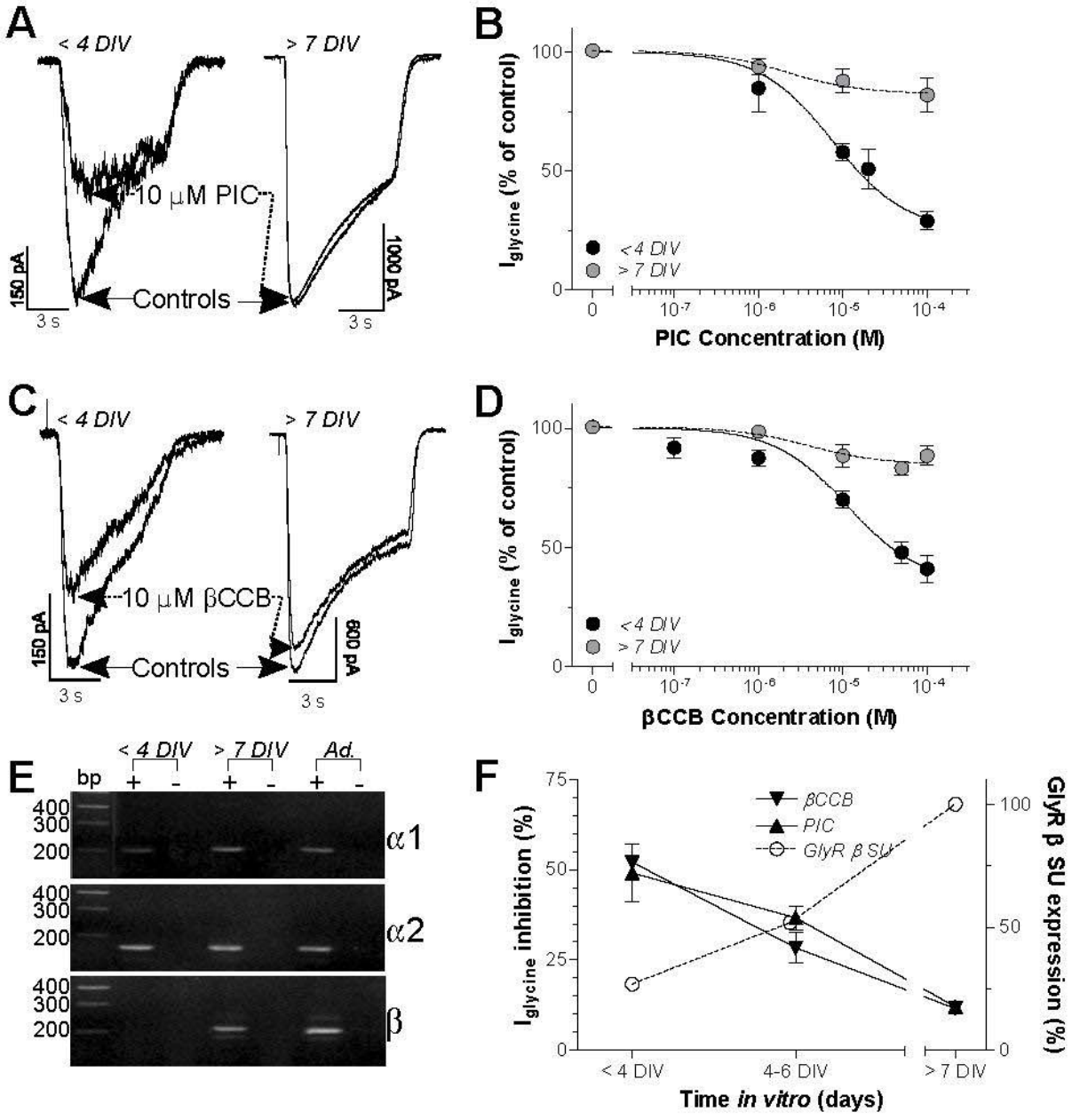

Molecular Pharmacology Fast Forward. Published on February 18, 2005 as DOI: 10.1124/mol.104.007435
This article has not been copyedited and formatted. The final version may differ from this version.

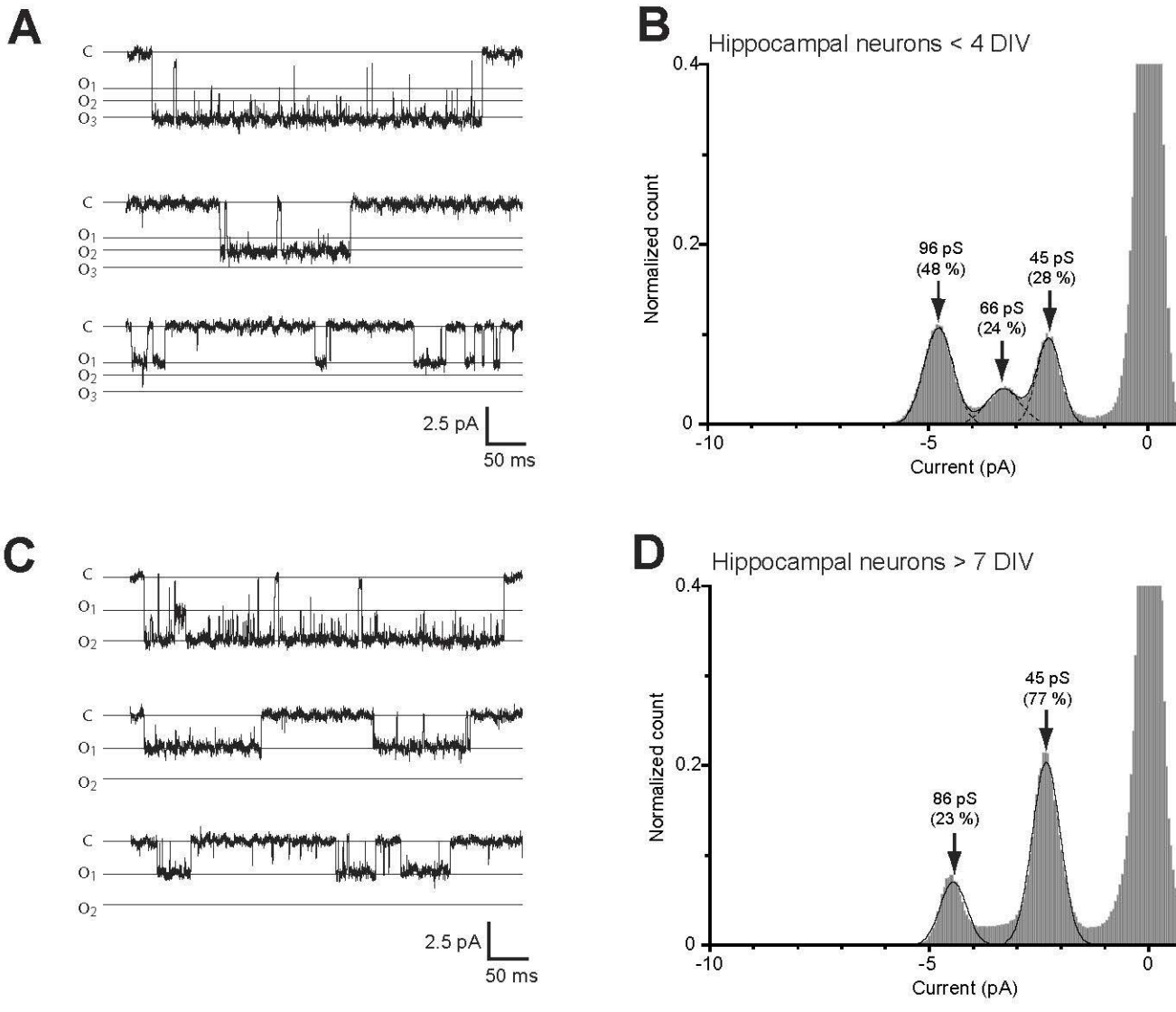

Molecular Pharmacology Fast Forward. Published on February 18, 2005 as DOI: 10.1124/mol.104.007435
This article has not been copyedited and formatted. The final version may differ from this version.

Figure 5

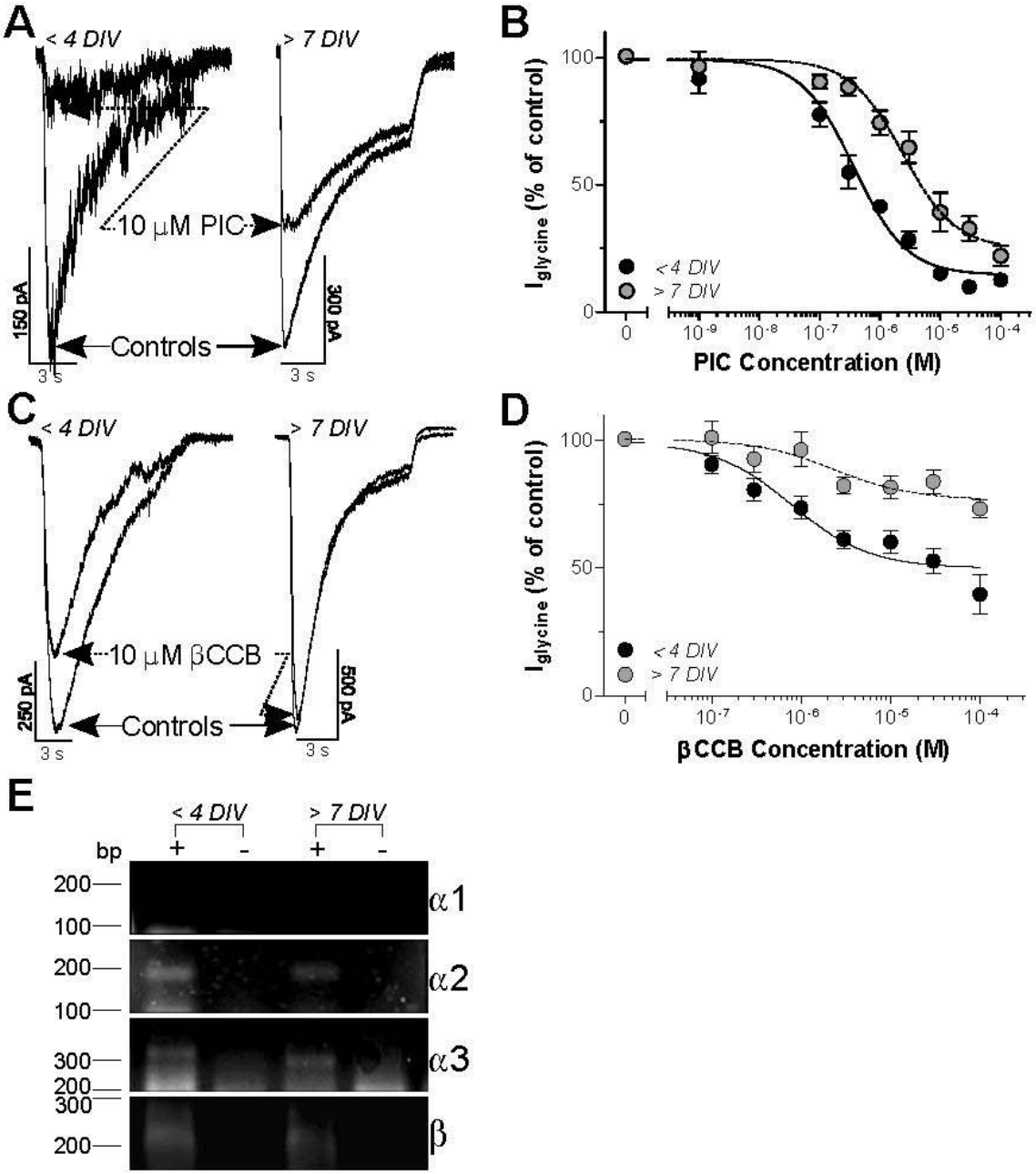

Molecular Pharmacology Fast Forward. Published on February 18, 2005 as DOI: 10.1124/mol.104.007435
This article has not been copyedited and formatted. The final version may differ from this version.

Figure 6

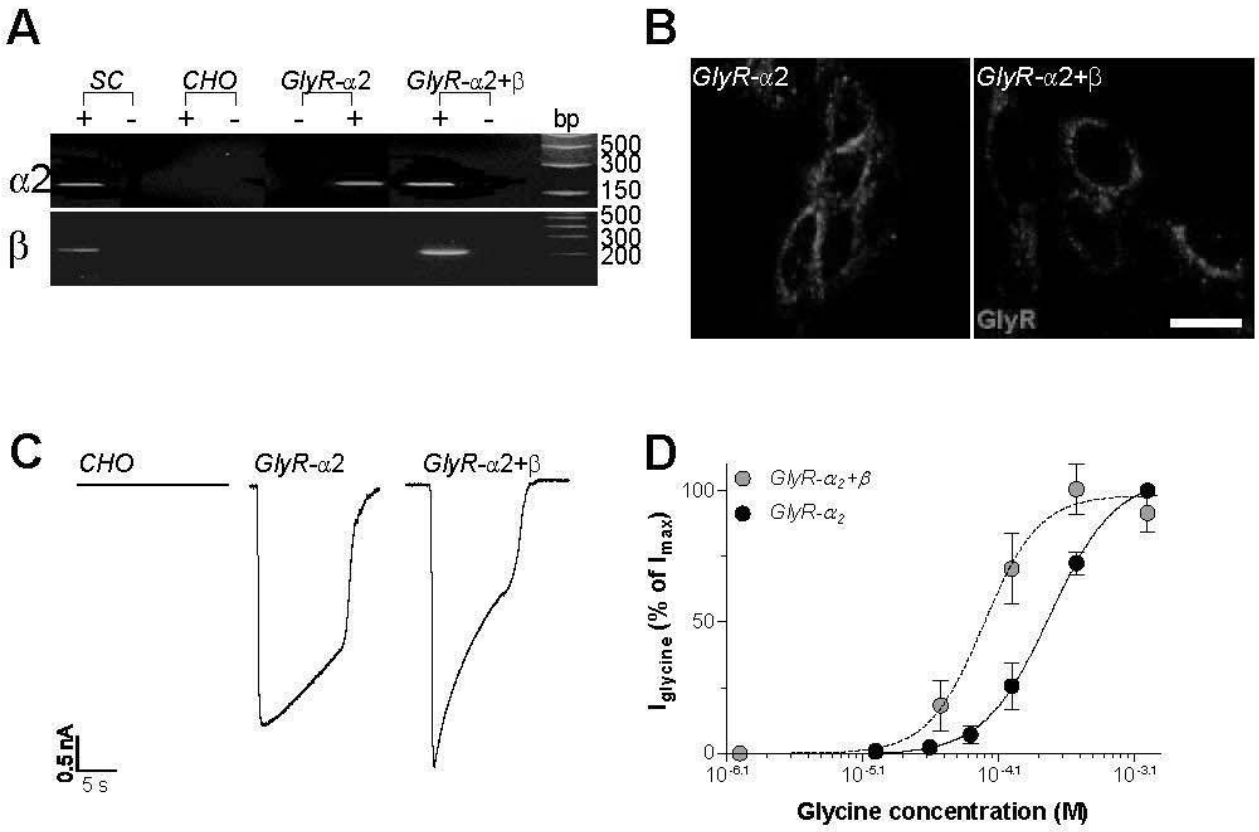

Molecular Pharmacology Fast Forward. Published on February 18, 2005 as DOI: 10.1124/mol.104.007435
This article has not been copyedited and formatted. The final version may differ from this version.

Figure 7

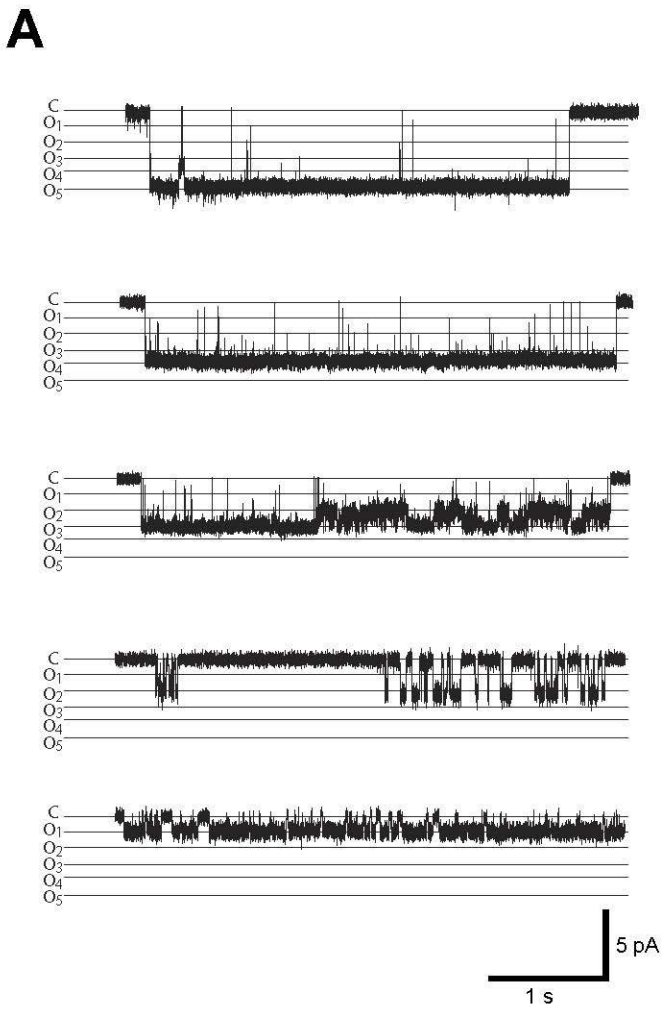

Molecular Pharmacology Fast Forward. Published on February 18, 2005 as DOI: 10.1124/mol.104.007435
This article has not been copyedited and formatted. The final version may differ from this version.

Figure 8